5-2021

An Examination of Grid Stability as it Relates to the Increased Integration of Inverter-Based Resources

Daniel Voss

An Examination of Grid Stability as it Relates to the Increased Integration of Inverter-Based Resources

A thesis submitted in partial fulfillment
of the requirements of the degree of
Honors Bachelor of Science in Electrical Engineering

by

Daniel Voss
University of Arkansas
Bachelor of Science in Electrical Engineering, 2021

May 2021
University of Arkansas

This thesis is approved for recommendation to the Honors College.

_____

Dr. Roy McCann, PhD., P.E.
Honors Thesis Advisor

Abstract

There is currently a growing interest in increasing the amount of renewable energy resources connected to the bulk electric system (BES) that stems from various environmental, political, and social concerns. However, the differences between conventional generation resources and inverter-based resources (IBR)—namely wind and solar—pose new issues that make this increased integration a larger problem. In other studies, the increased penetration of renewable energy resources has resulted in weak-grid systems that are more susceptible to collapse. This comes as a result from the inability for IBRs to effectively provide enough reactive power, an effect especially apparent during fault conditions, which the National Electric Reliability Council (NERC) requires utility companies simulate and test. This paper seeks to examine the problems surrounding the stability of the grid as increased renewable integration changes the impedance profile of the system as a whole. By beginning with a minimized 6-bus system based on the standard IEEE 14-bus system model, a comparison between current grid topologies and IBR-rich topologies is made and preliminary conclusions drawn. These conclusions are followed by a discussion of potential future work and possible other solutions to the problems faced during the study.

Acknowledgment:

I would like to thank Dr. McCann for his support for the past 4 years, both academically and professionally. He sparked my interest in the grid and pursuing renewable energy as a career. I would like to thank Doug Bowman for providing me with “real life” data and support through two summer internships. That thanks is also extended to Southwest Power Pool for allowing me to work with them on various projects over the years. Finally, I would like to thank my family and friends, without whose constant and continued support I would not be the man I am today.

Table of Contents

List of Figures

List of Tables

I. INTRODUCTION

The American bulk electric system (BES) is currently made up of a diverse collection of generation sources and load sinks. These sources are predominantly composed of conventional fossil fuel burning power plants that are able to supply loads with their required demand very reliably. The past few decades, however, have seen a notable shift toward increasing the amount of renewable energy resources—wind and solar most notably—to provide electricity for the consumer. This desire for cleaner electrical generation is motivated by environmental, social and political concerns and is incentivized to big utility companies through the use of tax credits and generation goals put in place by the American government [1].

The corporate and social benefits of increasing the amount of renewable generation plants within a company's footprint have driven many groups to begin widespread renewable integration projects. However, these new installations cannot serve as identical replacements for conventional generation sources. Renewable energy resources today require inverters to effectively connect to the larger grid. These inverter-based resources (IBRs) have a different impedance profile and different power limitations than conventional generators, thus having a discernable impact on the grid. When beginning one of these renewable energy projects, companies must spend many hours studying the influence of each new IBR plant. One of the primary concerns with the increased number of IBRs is the ability of the grid to maintain voltage stability. This paper seeks to examine the effects of a primarily IBR focused grid on voltage stability during system intact conditions and a contingency event.

A. Voltage Stability in General

Before examining the direct impact of IBRs on the electric power grid, it is important to have an adequate background on voltage stability in general. Voltage stability is the electric system's ability to maintain voltage while load power changes [2]. If the load's power requirements increase, the system must able to supply additional power without drastic changes in bus voltages in order to remain stable. Power requirements include both active and reactive components. Stability takes line losses into account; therefore, if a bus requires a certain amount of power at one end of a transmission line, the power consumption of the line must be known to yield a balanced system.

Oftentimes, reactive power compensation is used to maintain the voltage at the load. Doing so allows the load power to be increased. For this reason, reactive power compensation is frequently an alterable variable within the power system, with switching components allowing varying degrees of reactive compensation to be applied at different times. That being said, in a situation where the load power has been increased and a voltage instability event occurs, this compensation may not be enough and collapse could be more likely due to the presence of additional load. Voltage collapse is usually a culmination of several voltage instability events that cause equipment switching, generator tripping, tap changes, and even operator actions to behave abnormally in an effort to once again supply adequate power to the load [3]. Following voltage collapse, it can take minutes or hours to correct the system which could pose a large issue for the customer.

The ability to maintain voltage stability or effectively recover after a voltage event has often been referred to as voltage security [2]. It is the goal of any system operator to maintain high levels of voltage security. Because voltage stability is not a clearly defined value, it is oftentimes classified in terms of margin—that is, the amount of additional load that can be supported, the

amount of increased system impedance that can be stayed or the severity of a voltage event that can be withstood. System planning is a large part of maintaining high levels of system security. Minimizing transmission line congestion and ensuring that additional generation is available at a moment's notice are just two of the ways that utility companies ensure the grid operates reliably. That being said, no plan is foolproof, and widespread changes in the grid require more studies to be performed. The following sections examine the influence of these new resources on the current electrical grid and how one can estimate the magnitude of this influence.

B. Grid Stability

Grid stability is defined as the ability of grid-connected generators to supply the required active and reactive power to grid-connected loads. In this way, a grid can maintain stability by constantly providing the power that is being requested and actively adjusting power output based on changes in load. In the United States, power is transferred through the grid at a frequency of 60 Hz. All of the generators and motors that are connected to the grid are therefore synchronized at this frequency, working together to service whatever load is needed at any given moment.

Perhaps the best way to visualize grid stability is to examine the P-V curve of the system, an example of which is given in Figure 1. The P-V curve shows the relationship between load power (P_L) and load voltage (V_L) under constant impedance (X_{Th}) and reactive power (Q_L). The shape of the curve can also be altered by changes in impedance and reactive power, as exhibited by changing reactive power Q in Figure 2. In order to maintain stability, the BES must operate on the top (blue) portion of the curve. The right-most tip of the curve represents the maximum loadability (or instability limit) of the system. As the characteristics of the grid change, the result of (1.1) [4] changes to affect the stability limit of the system as a whole. Sudden or very large changes can

push the operating point to the lower portion of the curve, resulting in voltage instability and possible collapse.

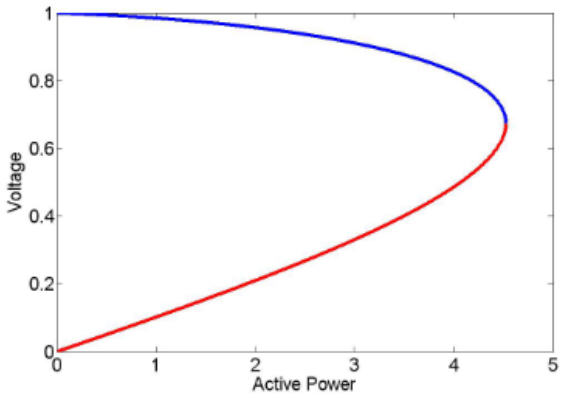

Figure 1. Example of a P-V curve of an electrical system, given to illustrate the regions of stability of a power system **[4]**

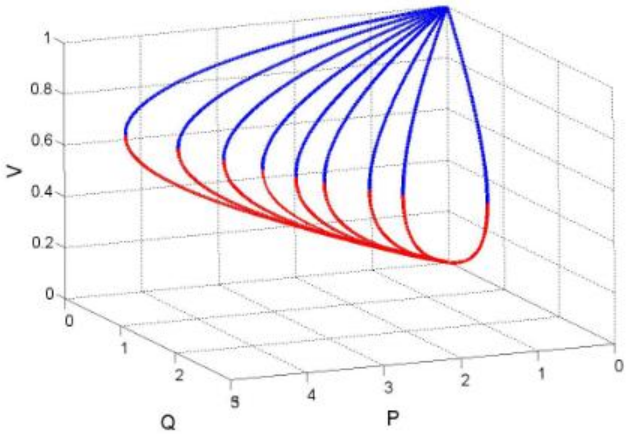

Figure 2. Example of several P-V curves where reactive power Q is also altered [4]

$$V_L = \sqrt{\frac{E_{Th}^2}{2} - Q_L X_{Th} \pm \sqrt{\frac{E_{Th}^4}{4} - X_{Th}^2 P_L^2 - X_{Th} E_{Th} Q_L}} \tag{1.1}$$

A fault can cause generation to be unable to keep up with load. This could look like a large generator suddenly failing, a load tripping offline for some reason or a transmission line becoming unusable. In any fault circumstance, the characteristics of the P-V curve change the point of

operation and could even change the shape. In severe instances, if the power requested by the load surpasses the maximum loadability, the voltage will begin to drop and with it, power. This inevitably causes voltage and frequency to sag. If the grid is unable to quickly provide additional generation, the instability event could increase in magnitude and load shedding (blackout) conditions might be warranted to protect equipment. Fortunately, most conventional generators are not run at their maximum output and can easily ramp up during a fault condition, rectifying the ratio of supplied to demanded power. This is not necessarily the case for IBRs that can operate on margin and lack a consistent 60 Hz signal.

1) Stability of Conventional Generators

All conventional turbine-based generators operate on the concept of inertia—the idea that an object in motion will remain in motion. The motion of all grid-connected generators is synchronized to a spinning 60 Hz signal. Because generator turbines have large masses, they tend to continue to spin at a frequency of around 60 Hz. Therefore, during a fault condition where another generator trips offline and is unable to produce more power, the rest of the generators will compensate by spinning slower, converting a portion of their rotational inertia into electrical energy in an effort to maintain the desired voltage. This action is relatively automatic and allows grid operators enough time to either ramp up current generators or bring new generators online. In this way, maintaining grid stability during fault conditions with conventional generators is easy as long as there is enough latent power available in the system to compensate any losses.

2) Synchronization and Stability of IBRs

Most IBRs do not naturally generate a 60 Hz voltage. Solar PV farms produce a dc signal that must be converted to ac at the appropriate frequency. The frequency of a wind turbine is highly dependent on the turbine type, rotor tilt, airspeed, among other variables. These devices can

therefore be very difficult to tie in to a synchronized grid and are typically synchronized using computation. This being the case, most grid connected inverters are operated as grid followers that track the phase angle and frequency of the grid using a phase lock look feedback system [5]. This fact is often overlooked in simulation studies, with simulations modeling IBRs as a conventional generator that can produce needed energy on demand. In reality, the output of renewable resources is very difficult to control directly, relying on environmental factors to provide limits to the amount of energy generated. During a fault condition, IBRs also lack the inherent spinning mass inertia seen in conventional generators to provide time for other generation to come online. Oversaturation of IBRs could there create a cascading failure effect, where, if a crucial spinning generator fails, the voltage and angle response of IBRs would not be able to respond fast enough to meet the required load.

Another significant issue with IBRs is their inability to produce large amounts of reactive power on demand. Reactive power generation is a characteristic that conventional generators have but is lost when using an inverter. It is true that IBRs are able to produce some reactive power. This power is derived from capacitors coupled with the inverter specifically for this purpose. However, these capacitors are of limited size and IBRs must operate within their reactive power limits. In the event that a limit is reached, IBRs must drop their terminal voltage to be able to continue providing needed power. Decreasing the voltage below normal terminal settings is not ideal, for it leads to underutilization of the resource. New technologies and programs have been designed to handle these issues at higher costs, both monetarily and in complexity [6], [7], [8].

A great deal of research has gone into the issue of synchronizing IBRs to the grid while maintaining stability. The issue of grid strength at different points of interconnect has been an area of great interest in both industry and academia, utilizing several methods to determine if injecting

IBR-based energy at certain points increases the likelihood of an instability event, [9], [3], [10]. Many methods focus on wind turbine generator type like the variable speed wind generators discussed in [11] or the double feed induction generators in [12]. Others consider IBRs to be voltage followers, adjusting their electronically controlled frequency and voltage quickly following a disturbance event, [5].

C. Proposed Solution

This research examines how an electrical system using exclusively IBRs will withstand a simple fault condition. A comparison between the power consumption and voltage stability of the system under system intact conditions and fault conditions will be made in an effort to show the importance of an IBR's ability to provide reactive power to uphold system stability. The study performed in this report is intended as a stepping stone toward future studies. The results presented here were generated on a simplified model whose intent was to imitate a larger power system; however, further investigation into the effects of widespread IBR use on larger systems is advised.

II. APPROACH AND METHODS

The following section outlines the approach and methods used to verify the theoretical response of the grid to changing IBR circumstances. It follows the development of the test model and derivations of the solution method—namely power flow solution through the Newton-Raphson solution strategy. Understanding this process will make analyzing the effect of high IBR penetration on voltage stability more straightforward. Reference [13] provided the equations given and was used as a guide in using them.

A. The Newton-Raphson Method

The Newton-Raphson solution method is one of the most common ways to solve power systems problems. It is an iterative method that uses matrices to solve a system of nonlinear algebraic equations. Rather than using "old values" during the iteration process like the Jacobi or Gauss-Seidel iterative methods, Newton-Raphson uses the Jacobian matrix composed of the partial derivatives of the equations to be solved. This solution method is used because it usually results in a fast convergence, meaning that the solution to the equations is found with minimal iterations.

Solving the Newton-Raphson equations for a power flow problem involves examining the phase angle δ, voltage V, real power P and reactive power Q at each bus. The per unit values of these variables are combined into the matrices shown below in (2.1) to (2.2). In the case of the system considered in this project, the N used is 6, representing the number of buses. It may be noted that the variables δ_1 and V_1 have been omitted from the equations. These represent the values for the swing bus which are already known. Convergence is determined by measuring the difference between y and the $f(x)$ elements, the latter of which is calculated during each iteration.

$$x = \begin{bmatrix} \delta \\ V \end{bmatrix} = \begin{bmatrix} \delta_2 \\ \vdots \\ \delta_N \\ V_2 \\ \vdots \\ V_N \end{bmatrix} \tag{2.1}$$

$$y = \begin{bmatrix} P \\ Q \end{bmatrix} = \begin{bmatrix} P_2 \\ \vdots \\ P_N \\ Q_2 \\ \vdots \\ Q_N \end{bmatrix} \tag{2.2}$$

$$f(x) = \begin{bmatrix} P(x) \\ Q(x) \end{bmatrix} = \begin{bmatrix} P_2(x) \\ \vdots \\ P_N(x) \\ Q_2(x) \\ \vdots \\ Q_N(x) \end{bmatrix} \tag{2.3}$$

The first step in the Newton-Raphson method is to calculate $f(x)$ using (2.4) and (2.5). These equations begin to use Y_{kn} and θ_{kn}, values from the admittance matrix of the system. The admittance matrix Y_{bus} is a matrix constructed from line and transformer data found within the model [13]. It is an N-by-N matrix that maps each connection between buses. The admittance matrix can be split into two separate matrices, one representing the magnitude Y of per unit admittance and one representing the corresponding angles θ. The diagonal elements of the admittance matrix Y_{kk} contain the sum of the admittances connected to the bus specified by k. The off-diagonal elements Y_{kn} represent the admittance connected between buses k and n. The setup for the θ matrix operates in the same way. With these matrices constructed, the following two equations can be solved and $f(x)$ can be filled in.

$$y_k = \mathrm{P}_k = \mathrm{P}_k(x) = \mathrm{V}_k \sum_{n=1}^{N} \mathrm{Y}_{kn}\mathrm{V}_n \cos\left(\delta_k - \delta_n - \theta_{kn}\right) \tag{2.4}$$

$$y_{k+N} = \mathrm{Q}_k = \mathrm{Q}_k(x) = \mathrm{V}_k \sum_{n=1}^{N} \mathrm{Y}_{kn}\mathrm{V}_n \sin(\delta_k - \delta_n - \theta_{kn}) \tag{2.5}$$

The next step is to construct the Jacobian matrix. A Jacobian matrix is a matrix consisting of the partial derivatives of a system of equations. In the case of a power system problem, the derivatives are taken as y with respect to x—in other words $\frac{d\mathrm{P}}{d\delta}$, $\frac{d\mathrm{P}}{d\mathrm{V}}$, $\frac{d\mathrm{Q}}{d\delta}$ and $\frac{d\mathrm{Q}}{d\mathrm{V}}$. Each of these derivatives make up one block of the completed Jacobian matrix, seen in (2.6) and (2.7). Each derivative shown in (2.7) has a corresponding equation given in Table 1. As can be noticed, there are differences between the diagonal and off-diagonal equations. These equations are derived from (2.3) and (2.4) above.

$$J = \begin{bmatrix} J_1 & J_2 \\ J_3 & J_4 \end{bmatrix} \tag{2.6}$$

$$J_1 = \begin{bmatrix} \frac{dP_2}{d\delta_2} & \cdots & \frac{dP_2}{d\delta_6} \\ \vdots & \ddots & \vdots \\ \frac{dP_6}{d\delta_2} & \cdots & \frac{dP_6}{d\delta_6} \end{bmatrix} \qquad J_2 = \begin{bmatrix} \frac{dP_2}{dV_2} & \cdots & \frac{dP_2}{dV_6} \\ \vdots & \ddots & \vdots \\ \frac{dP_6}{dV_2} & \cdots & \frac{dP_6}{dV_6} \end{bmatrix}$$

$$J_3 = \begin{bmatrix} \frac{dQ_2}{d\delta_2} & \cdots & \frac{dQ_2}{d\delta_6} \\ \vdots & \ddots & \vdots \\ \frac{dQ_6}{d\delta_2} & \cdots & \frac{dQ_6}{d\delta_6} \end{bmatrix} \qquad J_4 = \begin{bmatrix} \frac{dQ_2}{dV_2} & \cdots & \frac{dQ_2}{dV_6} \\ \vdots & \ddots & \vdots \\ \frac{dQ_6}{dV_2} & \cdots & \frac{dQ_6}{dV_6} \end{bmatrix} \tag{2.7}$$

Table 1. Jacobian Derivative Equations

Diagonals $n \neq k$
$J1_{kk} = \frac{dP_k}{d\delta_k} = -V_k \sum_{\substack{n=1 \\ n\neq k}}^{N} Y_{kn} V_n \sin(\delta_k - \delta_n - \theta_{kn})$
$J2_{kk} = \frac{dP_k}{dV_k} = V_k Y_{kk} \cos\theta_{kk} + \sum_{n=1}^{N} Y_{kn} V_n \cos(\delta_k - \delta_n - \theta_{kn})$
$J3_{kk} = \frac{dQ_k}{dV_k} = V_k \sum_{\substack{n=1 \\ n\neq k}}^{N} Y_{kn} V_n \cos(\delta_k - \delta_n - \theta_{kn})$ $J4_{kk} = \frac{dQ_k}{dV_k} = -V_k Y_{kk} \sin\theta_{kk} + \sum_{n=1}^{N} Y_{kn} V_n \sin(\delta_k - \delta_n - \theta_{kn})$
Off-Diagonals $n \neq k$
$J1_{kn} = \frac{dP_k}{d\delta_n} = V_k Y_{kn} V_n \sin(\delta_k - \delta_n - \theta_{kn})$
$J2_{kn} = \frac{dP_k}{dV_n} = V_k Y_{kn} \cos(\delta_k - \delta_n - \theta_{kn})$
$J3_{kn} = \frac{dQ_k}{d\delta_n} = -V_k Y_{kn} V_n \cos(\delta_k - \delta_n - \theta_{kn})$
$J4_{kn} = \frac{dQ_k}{dV_n} = V_k Y_{kn} \sin(\delta_k - \delta_n - \theta_{kn})$

Of particular note are $J2$ and $J3$. These equations represent the change in power, both active and reactive, with respect to voltage and have a direct relationship to the graph shown in Figure 2. Because $J2$ and $J3$ are derivatives, they represent the slope of Figure 2. During stable operation, the slope points gently downward. However, as voltage and admittance values change, this slope can be forced into a steeper and steeper position. If this derivative ever becomes undefined, the

system is operating at its instability limit and is at risk of becoming unstable. $J2$ and $J3$ are therefore important to monitor when monitoring for the stability of a system.

The results from Table 1 are inserted into (2.6) and the resulting matrix is used to back-solve for the change in δ and V . The values are then added to the previous values of δ and V to determine the next values. The entire process is then repeated until convergence is reached. In a power problem, convergence is reached when the Δy (where Δy is the change in P and Q from one iteration to the next) becomes smaller than some pre-determined value.

To simplify the process, the values for voltage-controlled buses can be eliminated because their V values are already known. This reduces the dimension of the Jacobian and thus can lead to convergence in less time. The values can also be left in the equations as long as the voltage value of the voltage-controlled buses are replaced after each iteration [13].

B. Model Design

A simplified test grid was developed to model the effects of increased IBR reliance on grid stability while maintaining a small enough solution set to be manageable. The system, shown in Figure 3, contains six buses, four of which are interconnected in a central grid. Bus 1 will serve as the swing bus, producing any extra power that may be needed. Three loads are connected to buses 2, 3, and 4. Two generators are connected to the grid through buses 5 and 6. These buses may represent either wind (bus 5) or solar PV farms (bus 6).

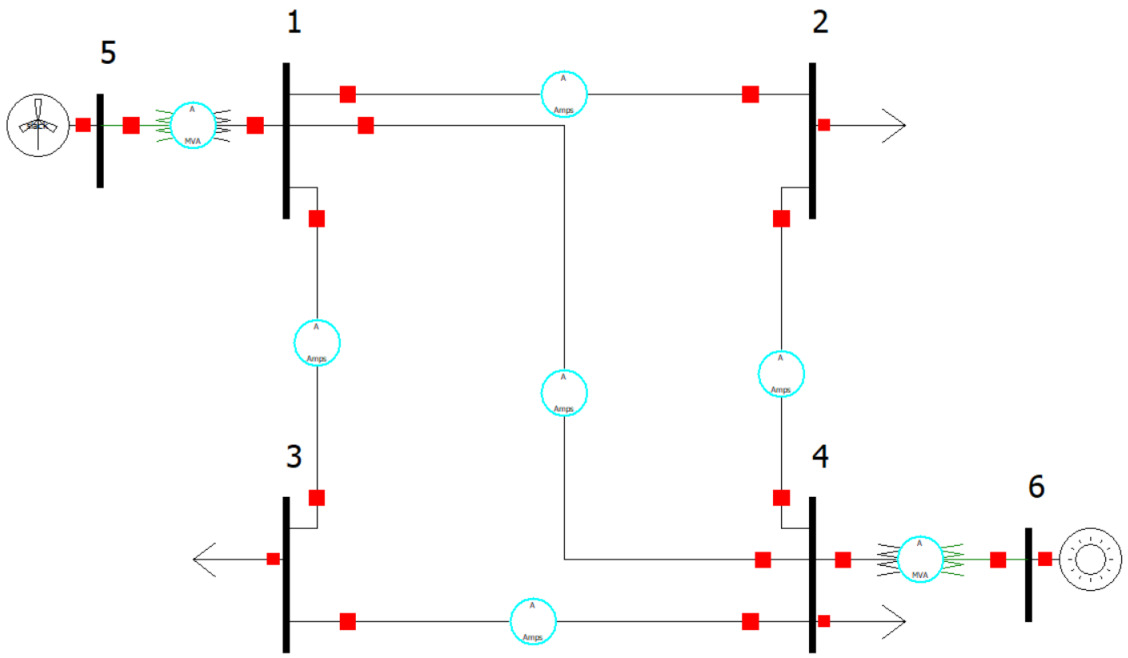

Figure 3. 6-bus weak grid IBR system used for testing

The transmission line impedance values—that is, the impedance values between buses 1, 2, 3 and 4—were selected from the IEEE standard 14-bus test system as modeled in [14] by the University of Illinois at Urbana-Champaign. The values shown in Appendix A were selected from buses with similar conditions (e.g. number of connected buses, associated loads and/or generators). The lines between buses 1 and 5 and buses 4 and 6 were chosen to model transformers, meaning the real values of their impedance were set to zero. The decision to make these lines transformers comes from the commonplace method of using a feeder bus/transformer combination to connect energy resources to the grid (example shown in Figure 4). The initial values for the IBR impedances were selected from a study being performed by Doug Bowman [15]. All impedances were converted to the per unit values using a base voltage of 138 kV and a base power of 100 MVA.

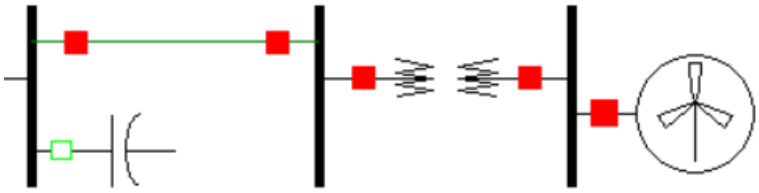

Figure 4. Example of typical point of interconnect for an IBR [15]

To fully examine the changes in grid stability due to the use of exclusively IBR impedance, the load and generation values will be changed throughout the study. The reactive power required by the system will be swept from an initially stable value into a range of instability. From there, the output of the IBRs will be manually altered to force the system back into the range of stability at the expense of underutilizing the resources. The change in active and reactive power produced by the IBRs will be noted and used to draw conclusions.

C. Model Implementation

The model from Figure 3 was implemented in MATLAB Simulink as a 3-phase grid system (shown in Figure 5). This model makes use of a modified PI design for modeling transmission lines (Figure 6), two winding 3-phase transformer blocks for modeling transformers, and a three-phase breaker for simulating a fault. The loads at bus 2 and bus 3 were selected to be general 3-phase parallel RL loads with adjustable power to simulate different conditions. The final load was constructed manually to allow for the internal impedance and power consumption to be easily altered (see Figure 7). The generation sources were chosen to be standard 3-phase sources with variable internal impedance. The impedance values were set to standard IBR impedance values as specified in [15]. The values of the generator impedance can be found in Appendix A.

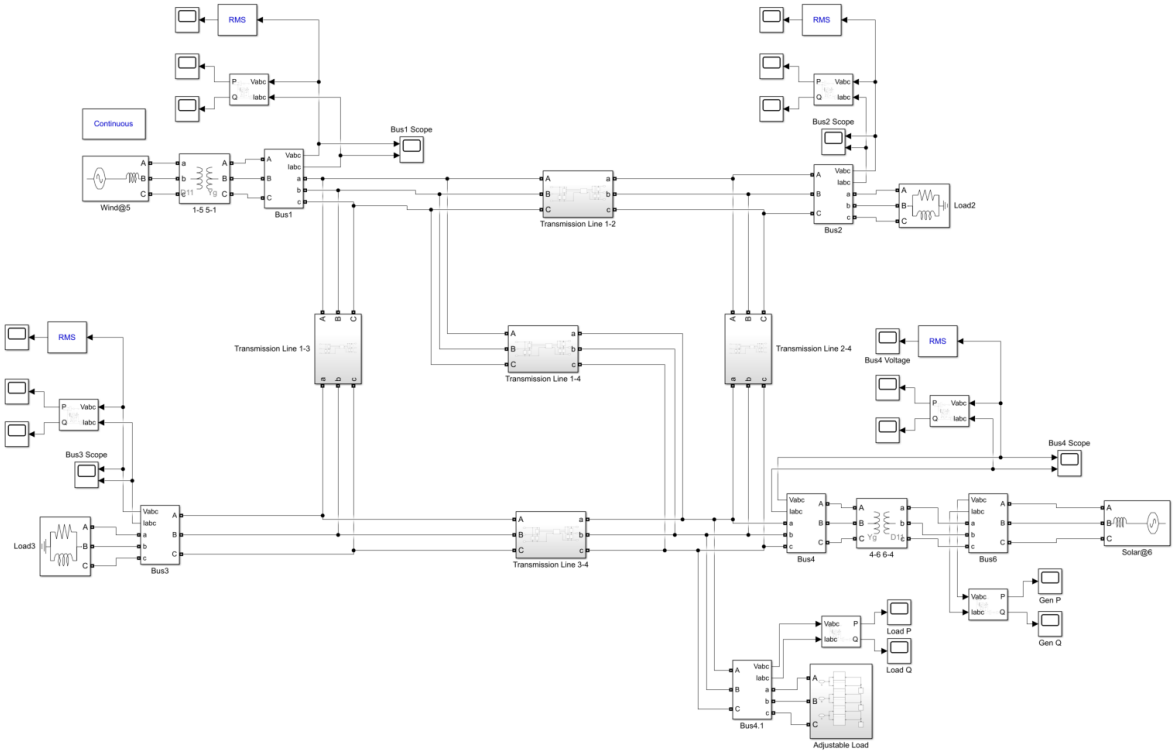

Figure 5. MATLAB Simulink 6-bus model

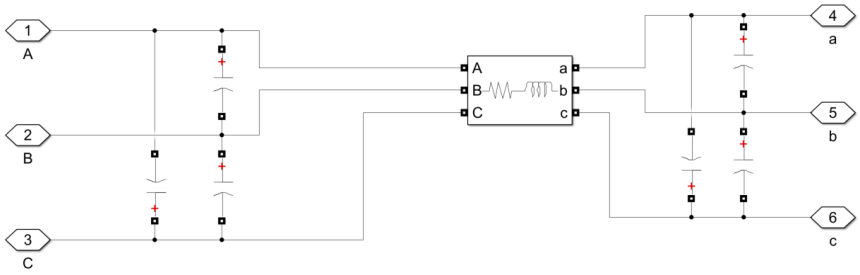

Figure 6. Modified PI design for modeling transmission lines

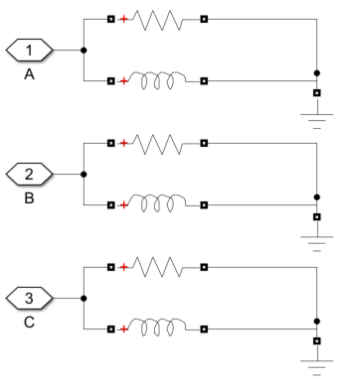

Figure 7. Modified load design used for adjusting parameters at load 4

The entire system is monitored with voltage, current and power scopes mapped to buses 1 through 4. During a fault, these scopes will reveal how each bus reacts to a changing grid system. Of particular note are the scopes at bus 4 where the load will be altered during testing.

D. Testing Methodology

The IBRs were stress tested by altering the power requirements of the system. Starting with a converging model, the reactive power of the load at bus 4 was increased until the solar IBR connected to the same bus exceeded the 25 MVAR limit. At that point, the output voltage of the IBR was dropped by 2% and the test was run at the same reactive power level before being increased again. In all, a total of 4 simulation schemes were tested. Two of the simulation schemes were performed under system intact conditions, one with the reactive power restrictions and the other without. The other two schema included a contingency (specifically tripping transmission line 1-4). These two simulations were also divided into requiring and ignoring reactive power limits. This combination of tests can provide an ample comparison between how an IBR-dense grid reacts during a contingency and with reactive power limits.

III. SIMULATION AND RESULTS

Testing was performed in two phases. The first phase of testing was performed during system intact conditions. This would serve as a baseline for the behavior of the system. Phase 1 was further divided into a test with and a test without IBR reactive power limits. The second phase of testing examined the system with an N-1 contingency—namely a 3-phase fault on the bus 1-4 transmission line. This test was also performed with and without IBR reactive power limits. The PV and QV curves of all four tests are discussed in the following subsections.

A. System Intact

System intact testing was performed to serve as a baseline comparison between the effect of IBR reactive power limits and unlimited reactive power generation. To best view the difference, the P-V and Q-V curves of the tests with and without the reactive power limits were plotted side by side. These can be seen in Figure 8 and Figure 9, where blue represents the test with limits and orange represents the test without limits.

For both simulations, the internal impedance of the load at bus 4 was decreased in 2% steps. This in turn increased the amount of power—both active and reactive—required by the bus. During the test without the reactive power limitation, the output of the IBR was kept at a constant 34.5 kV throughout the entire simulation set. This allowed the IBR to produce as much reactive power as was needed. During the test with limitation, if the generators output reactive power increased above the 25 MVAR limit, the IBR's output voltage was decreased by 2% in an effort to keep the IBR's reactive output within the limits. The IBR's output voltage was decreased until changes in voltage were unable to reduce the output reactive power below the specified limit. At this point, the IBR would no longer be able to function and the system would collapse if pushed further.

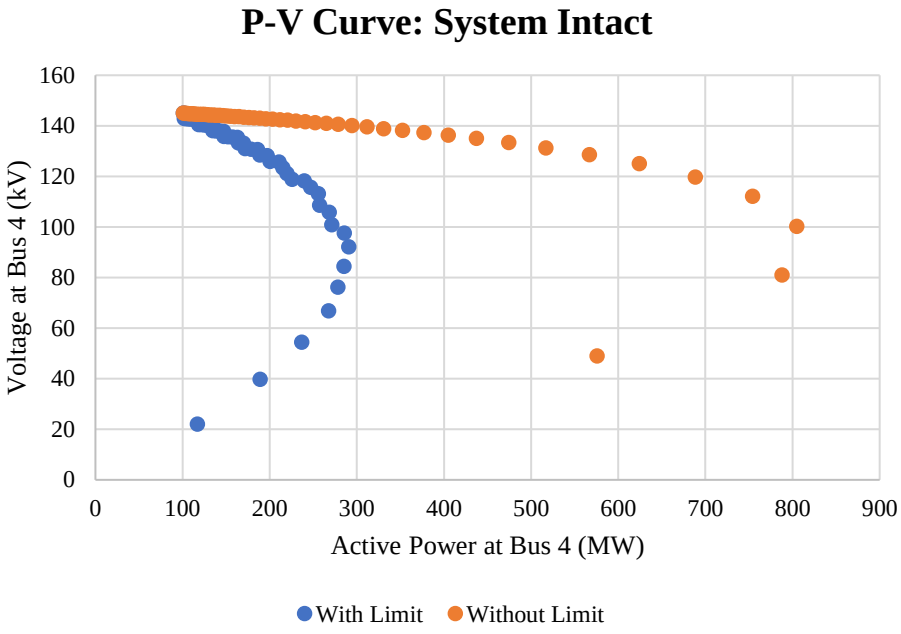

Figure 8. P-V curve of system intact simulations

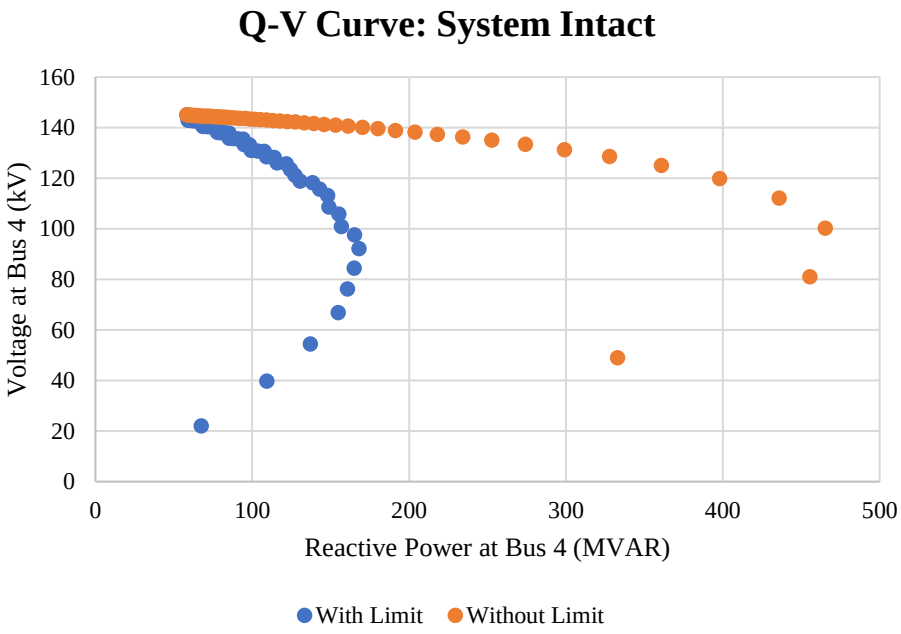

Figure 9. Q-V curve of system intact simulations

By plotting the P-V and Q-V curves for both situations, it quickly becomes clear that a generator without a reactive power limit is able to maintain stability for a substantially larger range of requested powers. Figure 8 and Figure 9 clearly show both the stable and unstable regions of

P-V and Q-V curve indicated by the example shown in Figure 1. The most striking difference between the results shown above is the disparity between the two. Both the active and reactive power curves of the limited IBR simulations fall far short of the simulations where the output was not limited. While an unlimited system, closely related to a more conventional generator, is shown to generate potentially up to 800 MW and 460 MVAR, the limited version can only produce up to about 280 MW and 165 MVAR, approximately 35% the output of the unlimited generator.

The results from the first simulation set suggest a similar pattern will be followed during the N-1 contingency phase, where conditions will be worse for maintaining system stability. This prediction will be examined next.

B. N-1 Contingency

The first set of simulations represent a sort of "best case" scenario where the system is not subject to any outages and is able to operate at its maximum capacity. However, in an effort to maintain reliability, NERC requires that utility companies simulate the effects of contingencies (faults) on their grid. These have the potential to fundamentally change the shape of the grid. Therefore, the limited and unlimited reactive power simulation sets ran above were also completed on the most detrimental N-1 contingency present in the tested model.

The test contingency was made up of a 3-phase fault on the bus 1-bus 4 transmission line that took place for 6 electrical cycles starting at 10/60 seconds. This was followed by a pair of breakers being thrown at 16/60 seconds, decommissioning that transmission line for the remainder of the simulation. An image of the contingency setup can be seen in Figure 10. This was chosen as the most critical outage because losing the direct link between bus 1 and 4 would further isolate the two generators in the simulation. Power from the slack bus (bus 5 IBR) would have to flow around

the fault through buses 2 and 3 in order to supply the load at bus 4 if the local IBR (bus 6 IBR) was unable to produce enough power.

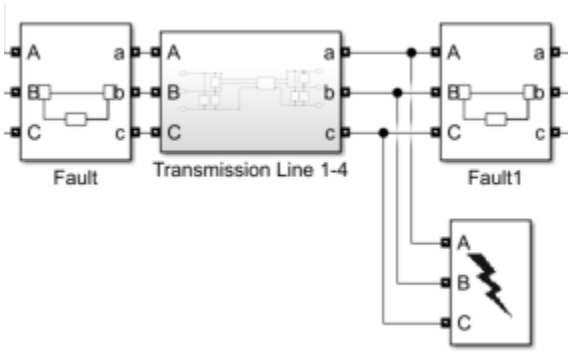

Figure 10. Contingency used for N-1 simulations

To test the impact of this contingency, the same set of tests were run on the system. In both cases, the load 4 impedance was stepped down in 2% intervals, allowing the load to require more active and reactive power. In one case, the IBR was allowed to generate an unlimited amount of reactive power; in the other, the IBR was limited to producing less than 25 MVAR. This limit was tested against the new steady state power requirements—that is, the power required after the fault was cleared. As was done before, the P-V and Q-V curves for both of these situations were plotted against each other, and the results can be seen in Figure 11 and Figure 12.

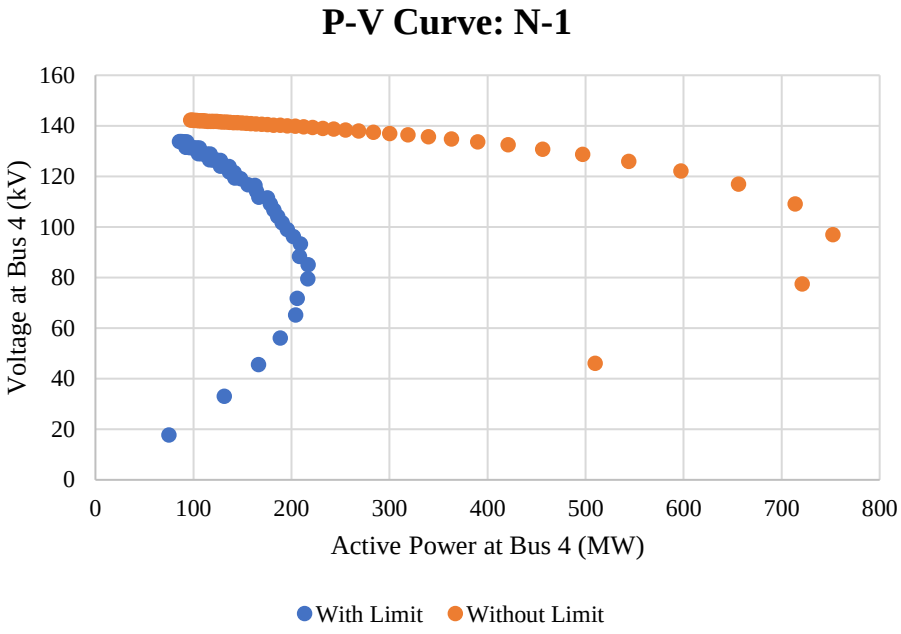

Figure 11. P-V curve of N-1 contingency simulations

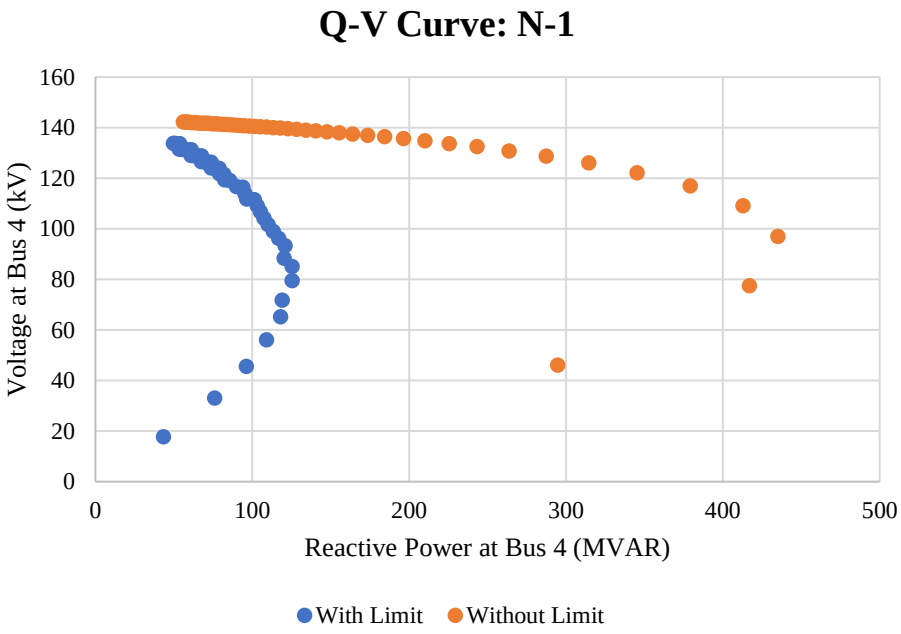

Figure 12. Q-V curve of N-1 contingency simulations

Once again, the reactive power limits on the IBR severely limited the amount of output power that could be produced. While the unlimited generator was able to produce up to 750 MW and 435 MVAR, the IBR was restricted to about 215 MW and 125 MVAR. In this circumstance, the IBR

was only able to produce 28% of what a more conventional generator could do. Given that this is an even lower portion than the system intact condition, the IBR became less reliable compared to a conventional generator during the worst-case N-1 contingency event.

The contingency demonstrated above is only an N-1 contingency that represents what happens when a single transmission line trips offline. In industry, contingency analysis is performed on important outages several orders higher than N-1. The reduction in load capacity provided by a single N-1 contingency was severe, but further reduction could be caused by compounding outages. For instance, if the transmission line from bus 3 to 4 fell out of service after the given contingency, power would then be limited to traveling through bus 2 to supply load 4. This would put more pressure on the IBR at bus 6, limiting load even further. In extreme events, the lack of IBR support could lead to load shedding in the event that demand increases past a certain point.

IV. CONCLUSIONS

This study has shown that IBRs lack the generational reliability inherent in more conventional generators. In a system containing only IBR generators, the reactive power limit of a single IBR significantly reduced the load capacity of the system in both system intact and worst-case N-1 contingency analysis. In both cases, the limitation placed on the IBR reduced load capacity at the POI bus by greater than 40%. In the real world, this limit could stunt load growth in certain areas or require additional equipment to provide support to IBRs during instability conditions.

The results given in this paper represent a tradeoff when it comes to IBR-based renewable generation as a whole. Although it is desirable to replace fossil fuel generators with solar farms and wind turbines, this transition may not be possible immediately. In an effort to design a greener grid, reliability and load capacity would have to be sacrificed. There have been some steps made

toward making this difficulty more sustainable. Research into control systems to improve IBR ride-through of disturbance events have been examined in [8]. Shunt capacitors have been used in similar applications to supply power factor correction and feed reactive power when needed [16]. There is even discussion of producing reactive power on-site [17] or integrating into PV plants themselves [18]. In any case, strides are being made in an effort to increase the feasibility of shifting electric grids around the world to more sustainable designs.

A. Future Work

The conclusions presented in this report were generated by simulating a simplified power system designed to effectively model the conditions present in a grid-scale system. There are, however, nuances that may be present in larger systems that would be difficult to test using a minimized bus system. It would therefore be prudent to test these results on systems of various sizes and using various pieces of software. This would serve to confirm the conclusion that IBR's are unable to provide reactive power support during system intact conditions and during N-1 contingencies.

An investigation into the effects of specific types of IBRs would also be highly beneficial. This report used a more generalized model of IBR admittances, commonly referring to them as "wind resources" but actually representing a general case. Although it is true that IBRs interact with the grid in very similar ways, every piece of equipment operates differently and an investigation into the influence of different type of IBRs using generation-specific admittance models could be beneficial to the planning process.

V. REFERENCES

[1] Energy Information Assosication, "Renewable Energy Explained: Incentives," EIA, 2020.

[2] C. Concordia, "Voltage Instability," in *Electrical Power & Energy Systems*, Venice, FL, Butterworth-Heinemann Ltd, 1991, pp. 14-20.

[3] A. M. Aldaoudeyeh, D. Wu and J. J. Jiang, "Identification of Critical Branches for Improving Weak Grid with Large-scale Integration of Inverter-based Resources," in *2019 IEEE Power & Energy Society General Meeting (PESGM)*, Atlanta, GA, 2019.

[4] S. Corsi and G. N. Taranto, "Voltage Instability - the Different Shapes of the "Nose"," College of Engineering Pune, Pune, India, 2007.

[5] D. Pattabiraman, R. H. Lasseter and T. M. Jahns, "Short-Term Voltage Stability of Power Systems with High Inverter Penetration under Small Disturbances," in *2019 IEEE Power & Energy Society General Meeting (PESGM)*, Atlanta, GA, 2019.

[6] J. Im, S. Kang, S. Song, S. Jung, J. Choi and I. Choy, "Reactive Power Control Strategy for Inverter-Based Distributed Generation System with a Programmable Limit of the Voltage Variation at PCC," in *International Conference on Power Electronics - ECCE Asia*, Jeju, South Korea, 2011.

[7] A. Dhaneria, "Grid Connected PV System with Reactive Power Compensation for the Grid," in *IEEE Power & Energy Society Innovative Smart Grid Technologies Conference (ISGT)*, Washington DC, USA, 2020.

[8] M. Basu, V. R. Mahindara, J. Kim and E. Muljadi, "Effect of High Penetrated Reactive Power Support Based Inverter-based Resources on the Power Stability of Microgrid Distribution System during Faults," in *2020 IEEE Industry Applications Society Annual Meeting*, Detroit, MI, 2020.

[9] D. Kim, H. Cho, B. Park and B. Lee, "Evaluating Influence of Inverter-based Resources on System Strength Considering Inverter Interaction Level," MDPI, Basel, Switzerland, 2020.

[10] D. Bowman, D. Ramasubramanian, R. McCann, A. Gaikwad and J. Caspary, "SPP Grid Strength Study with High Inverter-Based Resource Penetration," in *2019 North American Power Symposium (NAPS)*, Wichita, KS, 2019.

[11] M. Yagami, Y. Ichinohe, Y. Kojima, K. Misawa and J. Tamura, "Enhancement of Transient Stability of Synchronous Generators using Kinetic Energy of Variable Speed Wind Generators," in *2017 20th International Conference on Electrical Machines and Systems (ICEMS)*, Sydney, NSW, 2017.

[12] J. C. Munoz and C. A. Canizares, "Comparative Stability Analysis of DFIG-based Wind Farms and Conventional Synchonous Generators," in *2011 IEEE/PES Power Systems Conference and Exposition*, Phoenix, AZ, 2011.

[13] J. D. Glover, T. J. Overbye and M. S. Sarma, Power System Analysis & Design, Boston, MA: Cengage Learning, 2017.

[14] Illinois Center for a Smarter Electric Grid, "IEEE 14-Bus System," University of Illinois Board of Trustees, Urbana, IL, 2021.

[15] D. Bowman, "6Bus 138kV Test Casse33," SPP, Little Rock, AR, 2020.

[16] J. V. Schmill, "Optimum Size and Location of Shunt Capacitors on Distribution Feeders," *IEEE Transactions on Power Apparatus and Systems*, vol. 84, no. 9, pp. 825-832, 1965.

[17] J. Desouza, "Reactive Power Produced on-site Increasingly Important as Solar Power and EVs go Mainstream," 12 February 2020. [Online]. Available: https://pv-magazine-usa.com/2020/02/12/reactive-power-produced-on-site-increasingly-important-as-solar-power-and-evs-go-mainstream/. [Accessed 15 April 2021].

[18] S. Yee, "Reactive Compensation and Voltage Control with PV Generation Resources," Trimark Associates, Inc, Folsom, CA, 2015.

[19] D. Bowman, *Inverter-Based Resource Integration Study Results and Recommendations*, Little Rock, AR: Southwest Power Pool, 2020.

[20] S. Zhu, D. Piper, D. Ramasubramanian, R. Quint, A. Isaacs and R. Bauer, "Modeling Inverter-Based Resources in Stability Studies," in *2018 IEEE Power & Energy Society General Meeting (PESGM)*, Portland, OR, 2018.

[21] National American Electric Reliability Corporation, "United States Mandatory Standards Subject to Enforcement," NERC, 2021. [Online]. Available: https://www.nerc.com/pa/stand/Pages/ReliabilityStandardsUnitedStates.aspx?jurisdiction=United%20States.

[22] J. Sun, M. Li, Z. Zhang, T. Xu, J. He, H. Wang and G. Li, "Renewable Energy Transmission by HVDC Across the Continent: System Challenges and Opportunities," *CSEE Journal of Power and Energy Systems*, vol. 3, no. 4, pp. 353-364, 2017.

[23] NREL, "Renewables Rescue Stability as the Grid Loses Spin," NREL, 15 September 2020. [Online]. Available: https://www.nrel.gov/news/features/2020/renewables-rescue-stability-as-the-grid-loses-spin.html. [Accessed 2020].

[24] T. Van Cutsem, "Voltage Instability: Phenomena, Countermeasures, and Analysis Methods," *The IEEE*, vol. 88, no. 2, pp. 208-227, 2000.

APPENDIX A

Below are the values used for the transmission lines evaluated in this report. They were taken from the IEEE 14-bus system as provided by [14]. The values in Table 2 are given in engineering and per unit values.

Table 2. Transmission Line Parameters

Transmission Line	Resistance (Ω)	Inductance (H)	Resistance (p.u.)	Inductance (p.u.)
1-2	12.597	0.0658	0.06615	0.13027
1-3	32.551	0.1758	0.17093	0.34802
1-4	42.072	0.1009	0.22092	0.19988
1-5	0	0.1273	0	0.25202
2-4	18.087	0.1004	0.09498	0.19890
3-4	23.406	0.0787	0.12291	0.15581
4-6	0	0.1273	0	0.25202
Wind@5 (IBR1)	6.66e-4	1.841e-4	0.13582	0.03757
Solar@6 (IBR2)	1.05e-5	7.596e-5	0.00214	0.01550